CHAPTER 7

Porosity Estimation and Lithology Prediction

This chapter describes the porosity estimation and lithology prediction. The porosity calculation and lithology identification of the subsurface of Karewa field is important to understand the potential reservoir zone, structures and overall geological situation. Porosity is known at well locations from the porosity logs of Karewa-1 well but the porosity of the zones far from the well location is unknown. Similarly, the lithology can be predicted at the Karewa-1 well location by comparison of different well logs (gamma ray, density, resistivity, porosity, sonic, etc.), but it is difficult to predict the lithology far from well locations.

7.1 Porosity Estimation

Porosity is estimated from the relationship of the acoustic impedance and porosity logs. The acoustic impedance log was derived from the multiplication of the density and velocity logs. In this study, the P-wave log is used as velocity log which is corrected based on a sonic log calibration. Generally, the acoustic impedance log is used either as an input for the inversion algorithm to constrain the initial model building, or to create a relationship between porosity and acoustic impedance. After calculating the acoustic impedance inversion result for the data volume, the relationship between the effective porosity and acoustic impedance is used to model the inverted porosity.

The acoustic impedance log is plotted against the effective porosity log to obtain the relationship (Figure 7-1). This relationship is then used to calculate the inverted effective porosity model for the seismic volume. Figure 7-1 shows a crossplot of acoustic impedance and effective porosity. The color bar of this figure shows a trend of increasing acoustic impedance and decreasing effective porosity with depth. The crossplot shows a polynomial relationship between the acoustic impedance and effective porosity, and the relationship is expressed mathematically by the Equation 7-1.

$$x = 58.77 - (0.0128 * y) + (0.0000009 * y^2) \quad \text{……………………..……7-1}$$

x = Effective porosity in percentage (%)

y = Acoustic impedance in ((m/s)*(g/cc))

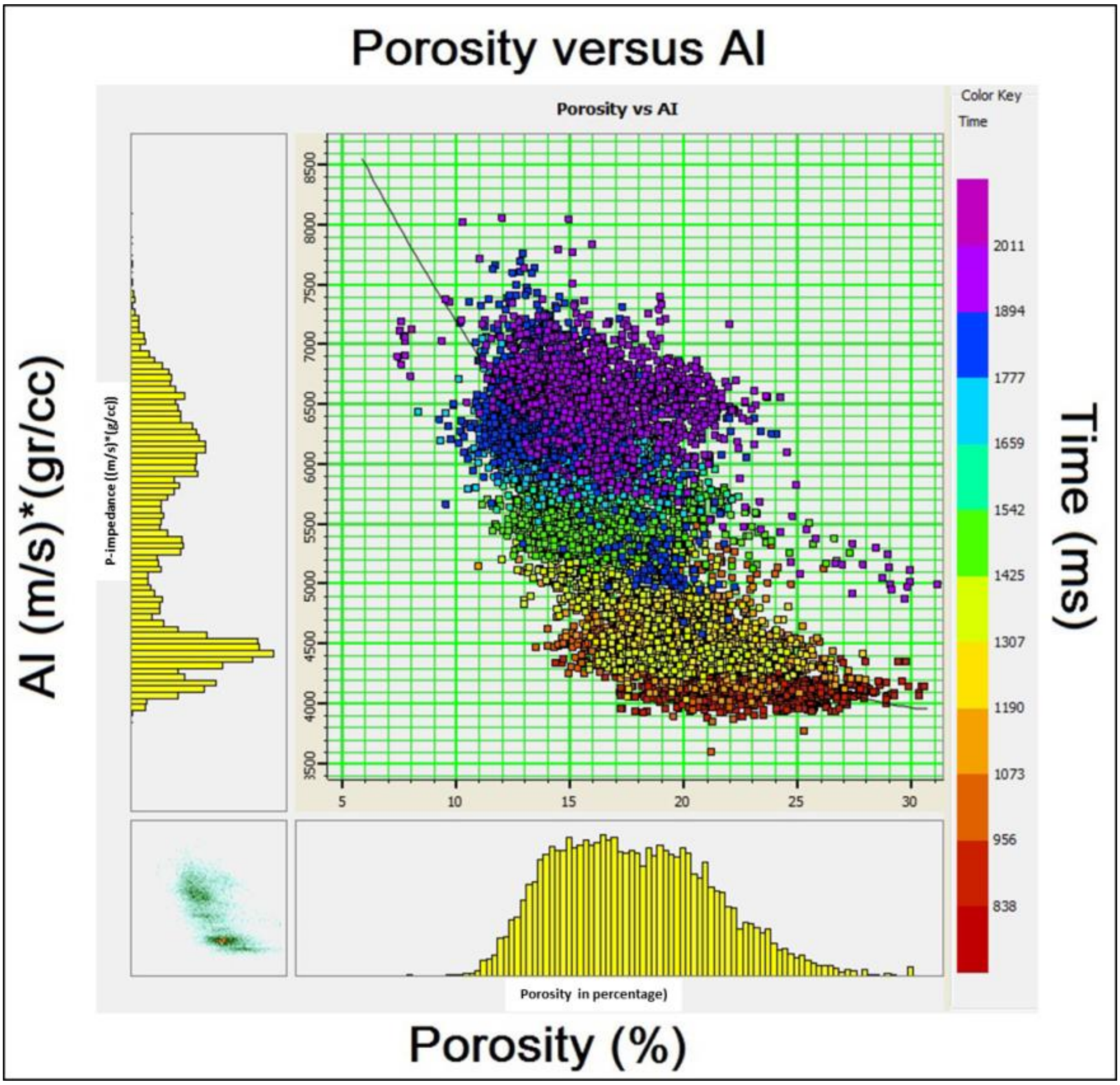

Figure 7-1: Acoustic impedance vs. effective porosity crossplot

Figure 7-2 shows the distribution of the inverted effective porosity on inline 1177. In Figure 7-2, H-1 shows low effective porosities, H-2 shows medium to high effective porosities, and H-3 shows medium effective porosity. H-4 shows high effective porosity in the central part (between crosslines 3380 and 4050) of inline 1177, and low to medium in other areas. H-5 has a medium effective porosity between crosslines 2880 to 3440 on inline 1177, and a low effective porosity in other areas. H-6 has a medium effective porosity between crosslines 2880 to 3230 on inline 1177, and a low effective porosity in other areas.

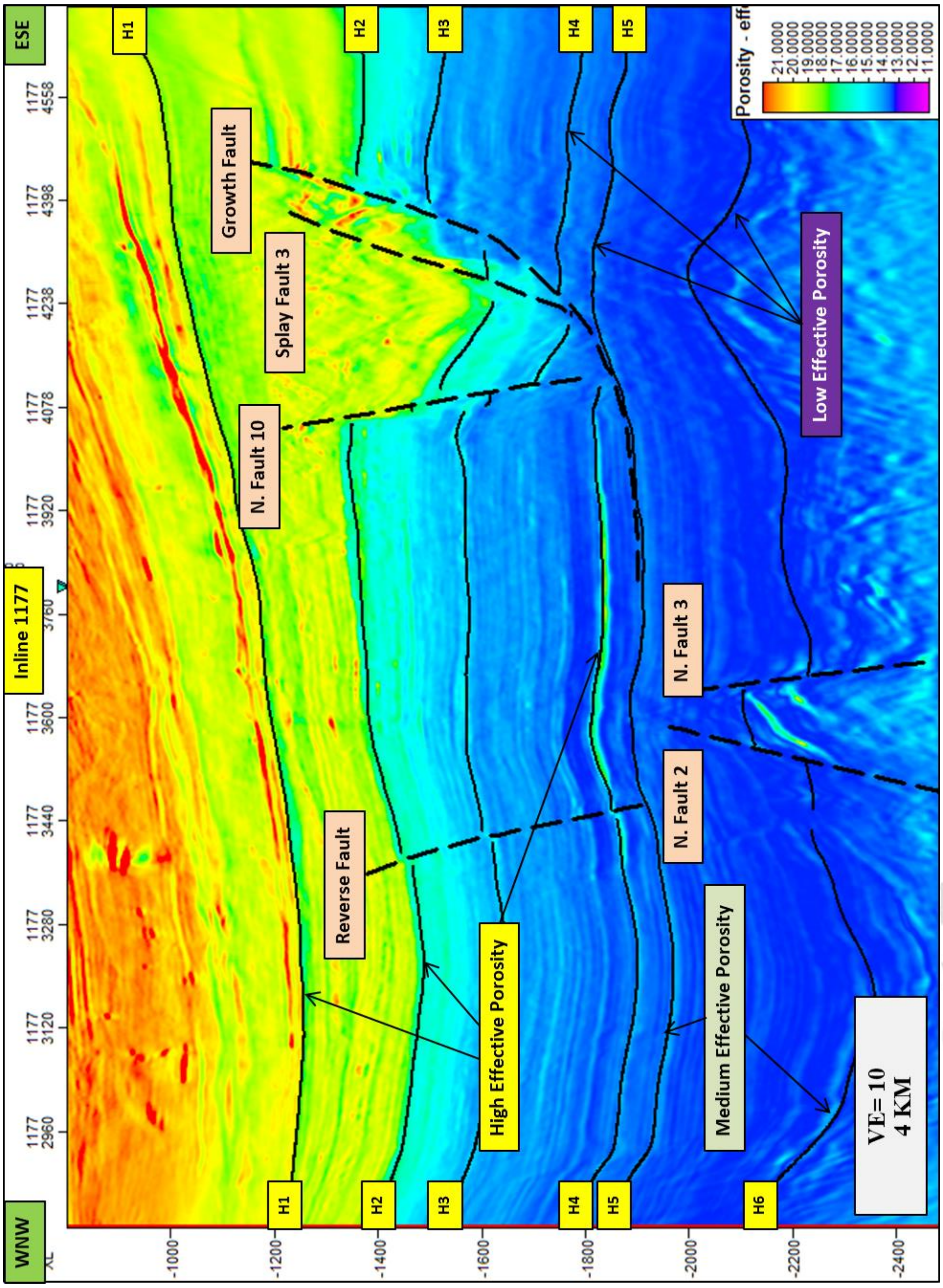

Figure 7-2: Inverted effective porosity distribution on inline 1177. Color bar shows the porosity distribution in percentage.

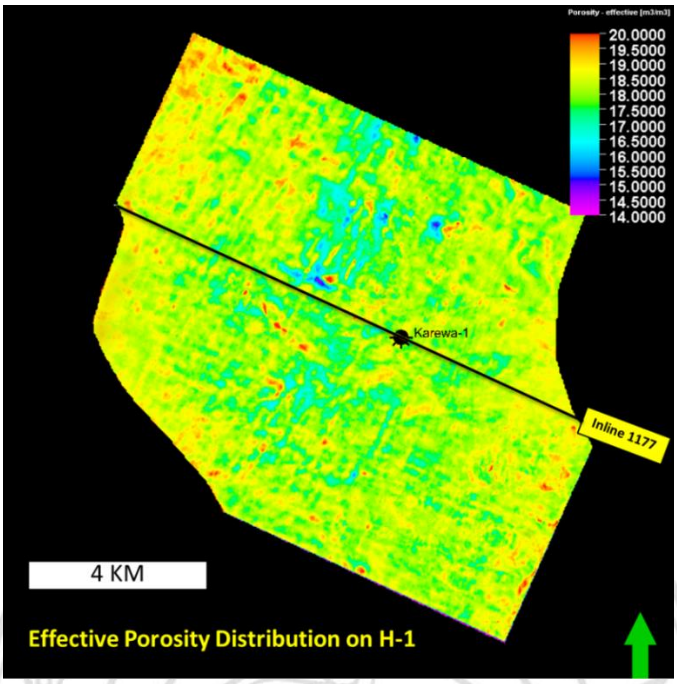

Figure 7-3: Inverted effective porosity distribution on H-1 surface

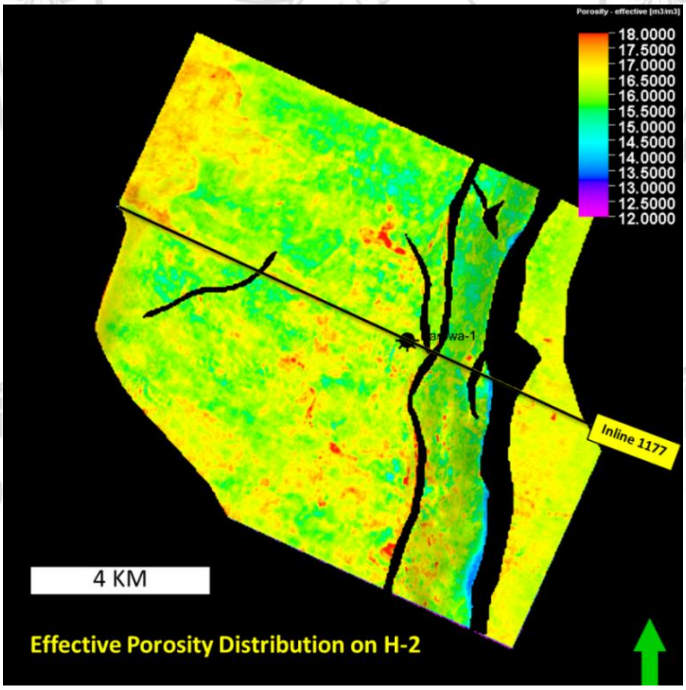

Figure 7-4: Inverted effective porosity distribution on H-2 surface

Figure 7-3 shows the inverted effective porosity distribution along H-1 with the porosity ranging from 14 to 20 percent. The lowest porosities occur in the center where the acoustic impedance was comparatively high (Figure 6-21). H-1 shows high predicted porosities as located in shallower zone.

Figure 7-4 shows the inverted effective porosity distribution along H-2 with the porosity ranging from 12 to 18 percent. Medium porosities are found in most of the study area except for the NW and the east. In the NW and east there are comparatively high predicted porosities ranging from 17 to 18 percent. The acoustic impedance is also low in these areas (Figure 6-22 and Figure 6-23). This can be related to lithology changes, as the porosity shows the same trend. This can be related to data acquisition and/or processing error.

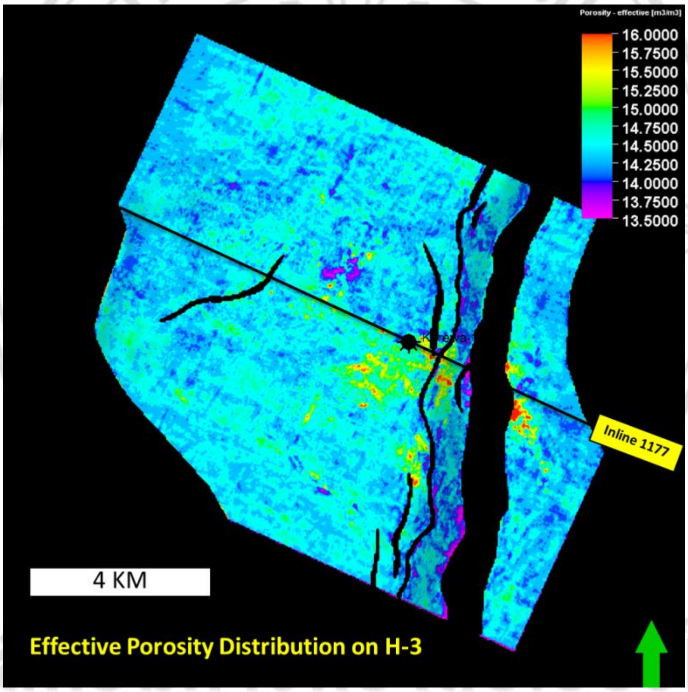

Figure 7-5: Inverted effective porosity distribution on H-3 surface

Figure 7-5 shows the inverted effective porosity distribution along H-3, with the porosity ranging from 13.5-16 percent. Porosities ranging from 13.5-14.5 percent characterize most of H-3 except for the central areas near the big faults. In central areas, there are comparatively high porosities ranging from 14.5-16 percent. The acoustic impedance is observed to be very low in this high porosity area (Figure 6-26). From the porosity distribution (Figure 7-5) and acoustic impedance (Figure 6-26) maps it can be interpreted that the central area is possibly containing hydrocarbon.

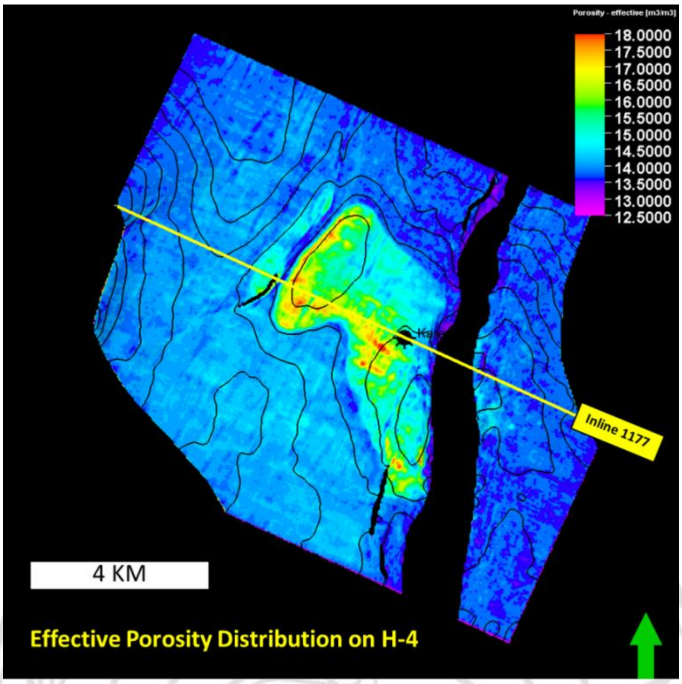

Figure 7-6: Inverted effective porosity distribution on H-4 surface

Figure 7-6 shows the inverted effective porosity distribution along H-4 with porosities ranging from 12.5-18 percent. Low porosity ranging from 12.5-14 percent characterizes the west, north and east of H-4. Porosity ranging from 14-14.5 percent marks the south and SW of H-4. Porosities is ranging between 14 to 18 percent characterize the central part of H-4. This central area of very high porosity is the gas saturated Mangaa C-1 Sand. The acoustic impedance values are found to be very low in this zone (Figure 6-29), whereas high RMS amplitude, envelope, and sweetness values are found (Figure 6-30 and 6-31). The observed effective porosity is 15 percent at the Karewa-1 well position and higher effective porosity can be observed near the high structure.

Figure 7-7 shows the inverted effective porosity distribution along H-5 with a porosity range between 12.5 and 14.5 percent. Low porosity from 12.5-13.8 percent are present in NE, East and SE. Comparatively medium range porosity between 13.8 and 14.5 percent occur in the NW, west and SW. The acoustic impedance is comparatively low in the NW and west of H-5 (Figure 6-32).

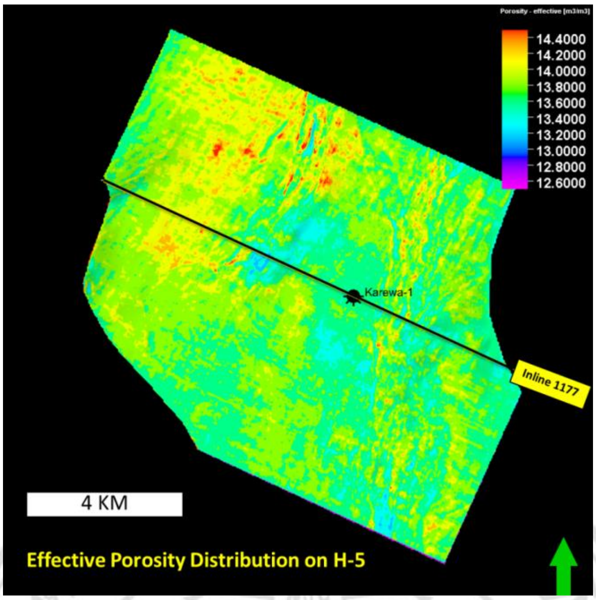

Figure 7-7: Inverted effective porosity distribution on H-5 surface

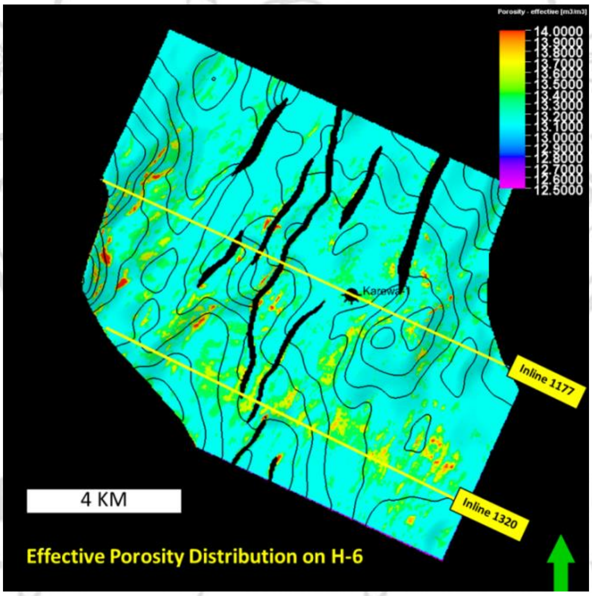

Figure 7-8: Inverted effective porosity distribution on H-6 surface

Figure 7-8 shows the inverted effective porosity distribution along H-6 with the porosity ranging from 12.5-14 percent. Very low porosities ranging from 12-13 percent are found along most of H-6 except for the south and SW. In the south and SW, porosity ranges from 13-14 percent and in this zone comparatively greater porosity values are predicted for several zones in which the acoustic impedance is also low and the RMS amplitude, envelope and sweetness values are high (Figure 6-35, 6-36, and 6-37). These changes are possibly related to the changes in lithology or compaction effects. Figure 7-2 shows the comparatively higher values porosity ranging from 13-14 percent between crosslines 2880 to 3230 on inline 1177 and the low effective porosity in the other areas. Figure 7-9 shows comparatively higher values of effective porosity ranging from 13-14 percent for H-6 on inline 1320. On the porosity map of H-6 (Figure 7-8), the positions of inline 1177 and inline 1320 are shown.

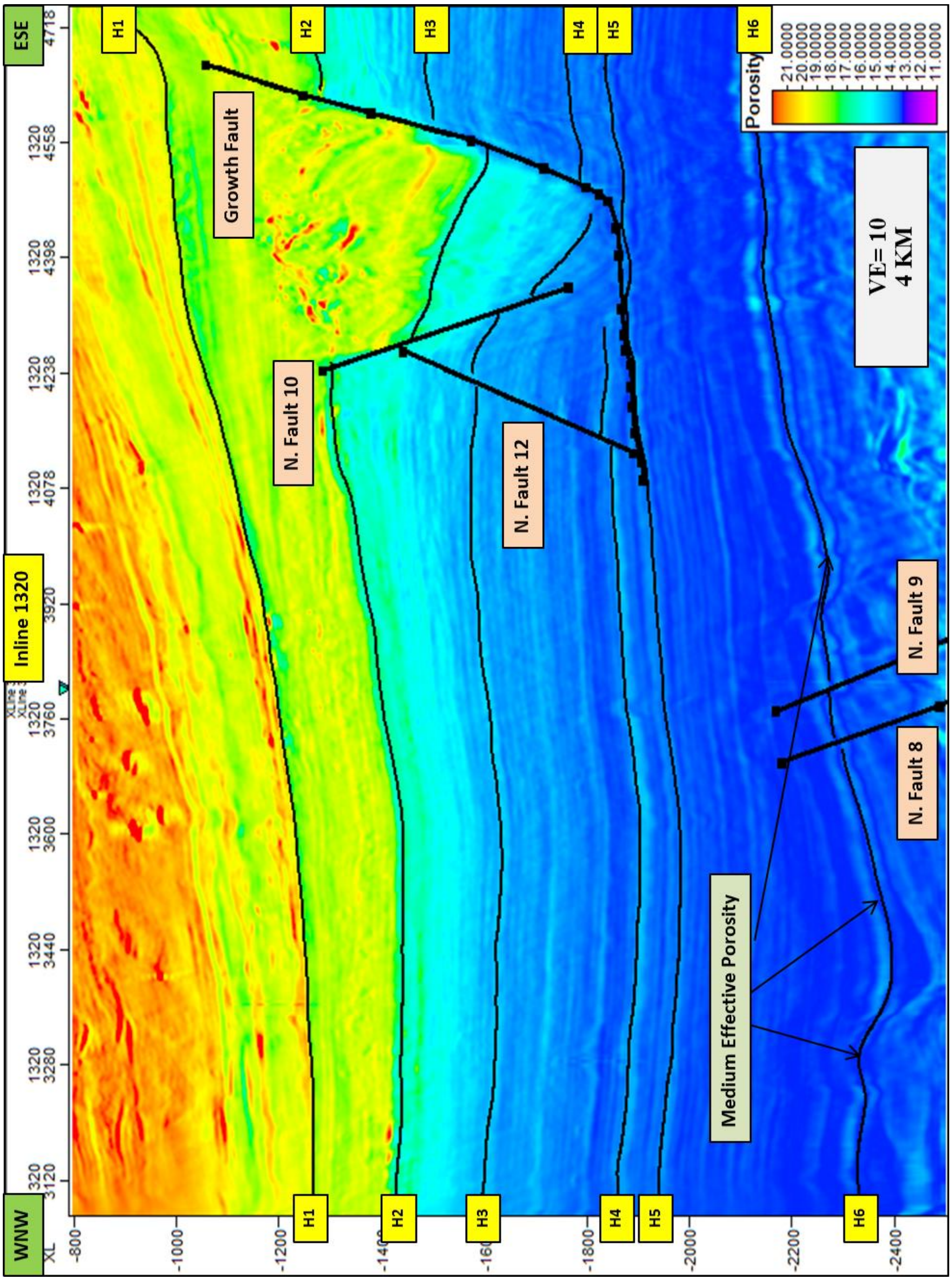

Figure 7-9: Inverted effective porosity distribution on inline 1320

7.2 Lithology Prediction

The lithology distribution is predicted for H-1 to H-6 using the gamma ray log, the inverted acoustic impedance distribution, and the inverted porosity distribution. The Karewa-1 well completion report (Conoco Northland Ltd., 2002-2003) is used to ground truth the inversion and predicted porosity based lithology interpretation at the well location. The predicted lithology of the horizons at the well location can be primarily verified by the gamma-ray log. The inverted p-impedance and porosity distribution maps can be interpreted to show the lateral change of lithology.

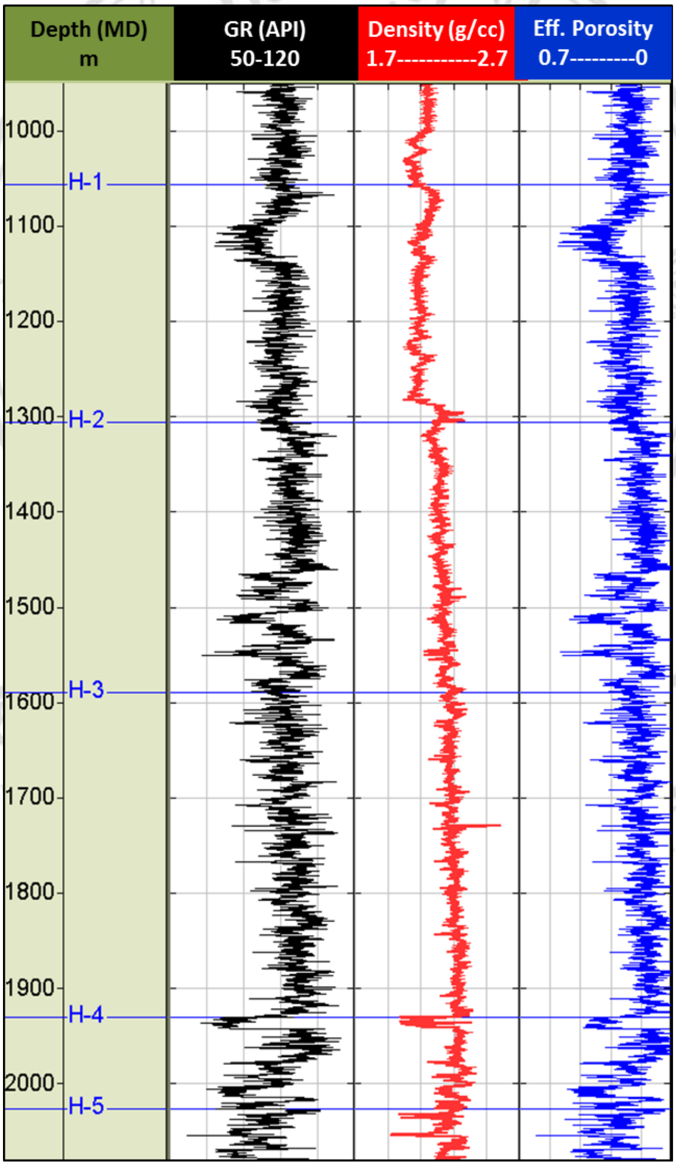

Figure 7-10: Gamma ray, density, and effective porosity logs show the log response for H-1 to H-5

H-1 was interpreted on a high negative amplitude reflection (trough) located at 1119ms TWT, which is 39ms TWT below the Plio-Pleist marker (1080ms TWT) of well karewa-1 (inline 1178). The depth is 1056m MD from the seismic-well tie. This depth is in claystone with sandstone interbeds according to the cutting sample descriptions of the Karewa-1 well completion report (Conoco Northland Ltd., 2002-2003). In Figure 7-10, the gamma-ray log shows high (90 API) value, the density log shows low (2.1 g/cc) value, and the porosity log shows 15% porosity at the intersection of H-1. These log values indicate claystone. Figure 7-11 shows the predicted distribution of claystone with medium acoustic impedance and medium predicted porosity. The other areas containing low acoustic impedance and high porosity probably consist of sandstone.

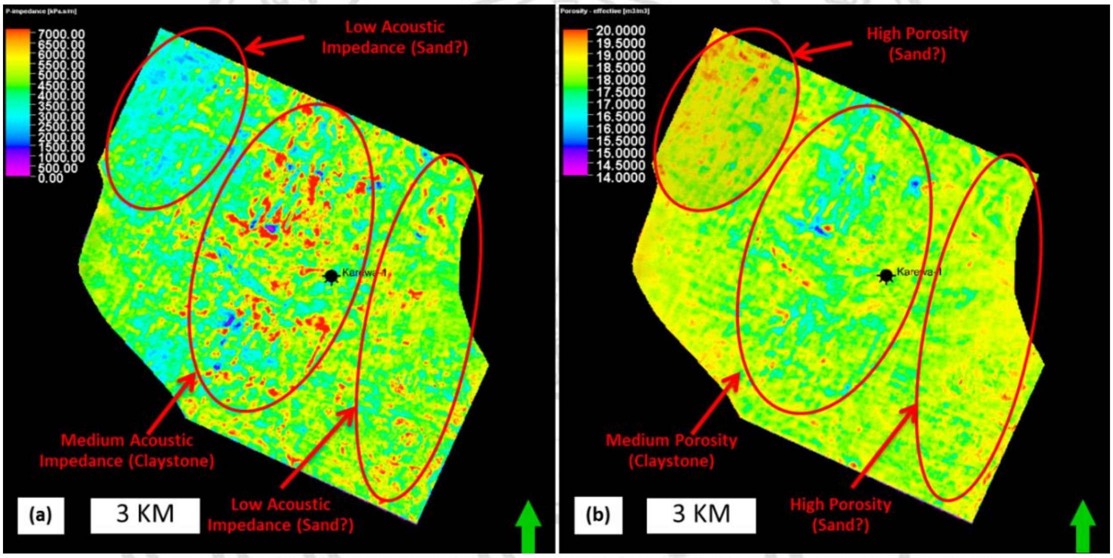

Figure 7-11: H-1 surface distribution maps (a) acoustic impedance, (b) porosity

H-2 was interpreted on a medium positive amplitude reflection (peak) located at 1345ms TWT, which is 15ms TWT below the Intra Giant Foresets marker (1330ms TWT) at well Karewa-1 (inline 1178). The depth is 1306m MD, as derived from the seismic-well tie. This depth is in claystone with sandstone interbeds according to the cutting sample descriptions of the Karewa-1 well completion report (Conoco Northland Ltd., 2002-2003). In Figure 7-10, the gamma-ray log shows high (93 API) value, the density log shows medium (2.25 g/cc) value, and the porosity log shows 13% porosity at the intersection of H-2. These log values indicate claystone. Figure 7-12 shows the predicted distribution of claystone with low to medium acoustic impedance and medium to high porosity. The other areas characterized by low acoustic impedance and high porosity probably contain sandstones, although there are some uncertainties because there might be acquisition and/or processing errors in the NNW and east.

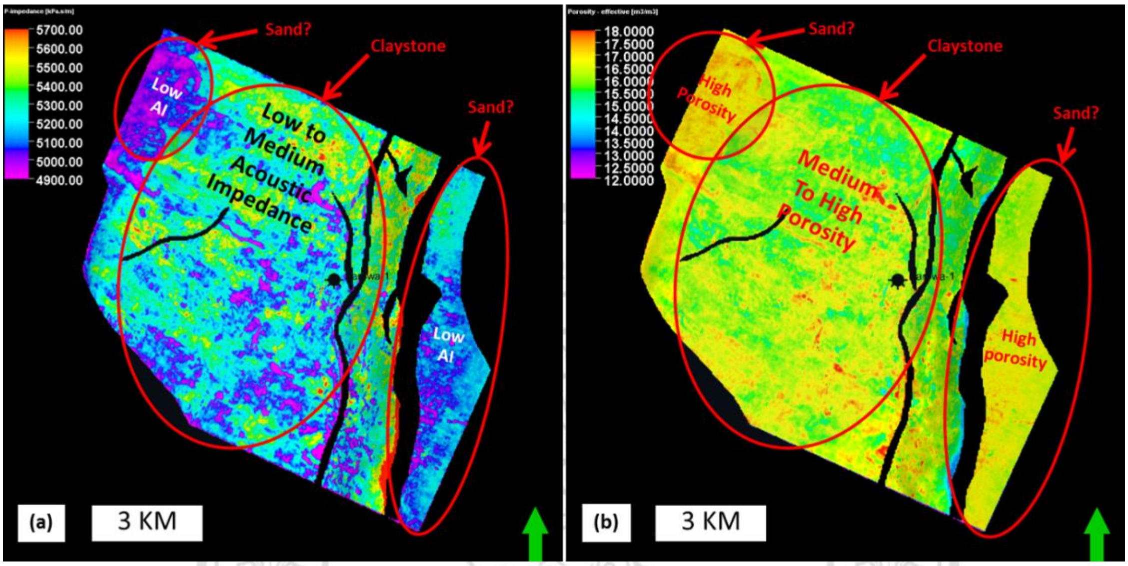

Figure 7-12: H-2 surface distribution maps (a) acoustic impedance, (b) porosity

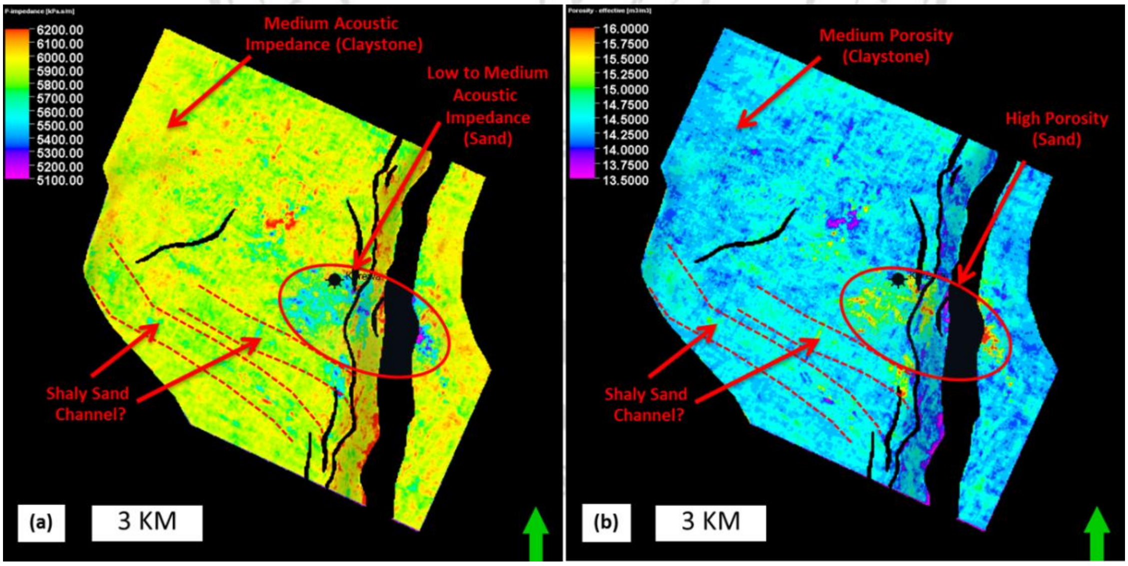

Figure 7-13: H-3 surface distribution maps (a) acoustic impedance, (b) porosity

H-3 was interpreted on a positive amplitude reflection (peak) located at 1571ms TWT at well Karewa-1 (inline 1178). The depth is 1589m MD, as derived from the seismic-well tie. This depth is in claystone with sandstone interbeds according to the cutting sample descriptions of the Karewa-1 well completion report (Conoco Northland

Ltd., 2002-2003). In Figure 7-10, the gamma-ray log shows high (95 API) value, the density log shows medium (2.3 g/cc) value, and the porosity log shows 10% porosity at the intersection of H-3. These log values indicate claystone. Figure 7-13 shows the predicted distribution of claystones with medium acoustic impedance and medium predicted porosity. Claystones cover most of H-3. A small area in the center of the map contains low to medium acoustic impedance and high predicted porosity. If this zone is interpreted as sandstone, there are some lateral discontinuities. Two channel shapes can be observed in the south with comparatively low to medium acoustic impedance and medium to high predicted porosity. These channels probably contain shaly sandstones.

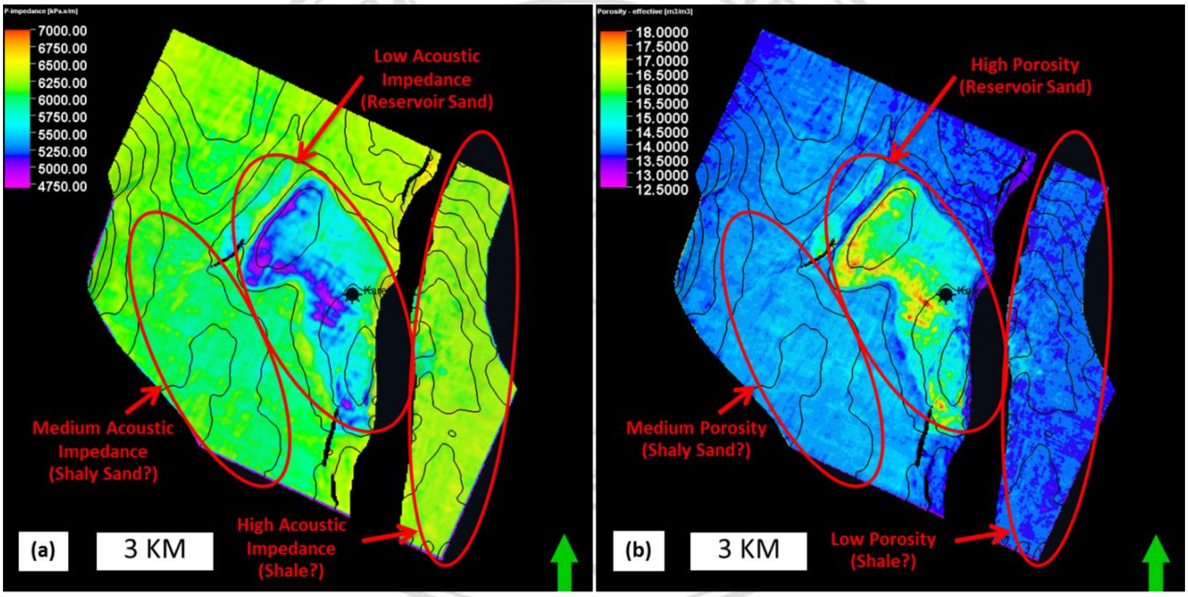

Figure 7-14: H-4 surface distribution maps (a) acoustic impedance, (b) porosity

H-4 was interpreted on a prominent positive amplitude reflection (peak) located at 1820ms TWT, corresponding to the Mangaa C-1 Sand marker at well Karewa-1 (inline 1178). The depth is 1930m MD, as derived from the seismic well tie and Karewa-1 well completion report (Conoco Northland Ltd., 2002-2003). H-4 is a reservoir rock confirmed by the core description and cutting sample description of the Karewa-1 well completion report (Conoco Northland Ltd., 2002-2003). In Figure 7-10, the gamma-ray log shows very low (68 API) value, the density log shows low (2 g/cc) value, and the porosity log shows 30% porosity at the intersection of H-4. These log values indicate hydrocarbon bearing sandstone. Figure 7-14 shows the distribution of the Mangaa C-1 Sand, characterized by very low acoustic impedance and high porosity.

The distribution of this reservoir sand covers the central area of H-4. The area in the south and SW containing medium acoustic impedance with medium porosity can be shaly sandstone. Other areas characterized by high acoustic impedance and low porosity are likely shales or claystones.

H-5 was interpreted on a positive amplitude reflection (peak) located at 1904ms TWT, which corresponds to the Intra Mangaa C-1 marker at well Karewa-1 (inline 1178). The depth is 2026m MD, as derived from the seismic-well tie and Karewa-1 well completion report (Conoco Northland Ltd., 2002-2003). H-5 corresponds to a claystone, which is confirmed by the core description and cutting sample descriptions of Karewa-1 well completion report (Conoco Northland Ltd., 2002-2003). In Figure 7-10, the gamma-ray log shows high (106 API) value, the density log shows medium (2.35 g/cc) value, and the porosity log shows 6% porosity at the intersection of H-5. These log values indicate shale or claystone lithology. Figure 7-15 shows the predicted distribution of claystones with medium to high acoustic impedance and low porosity. H-5 furthermore shows lateral lithology changes. Areas containing medium acoustic impedance and medium porosity can be possibly interpreted as shaly sandstones.

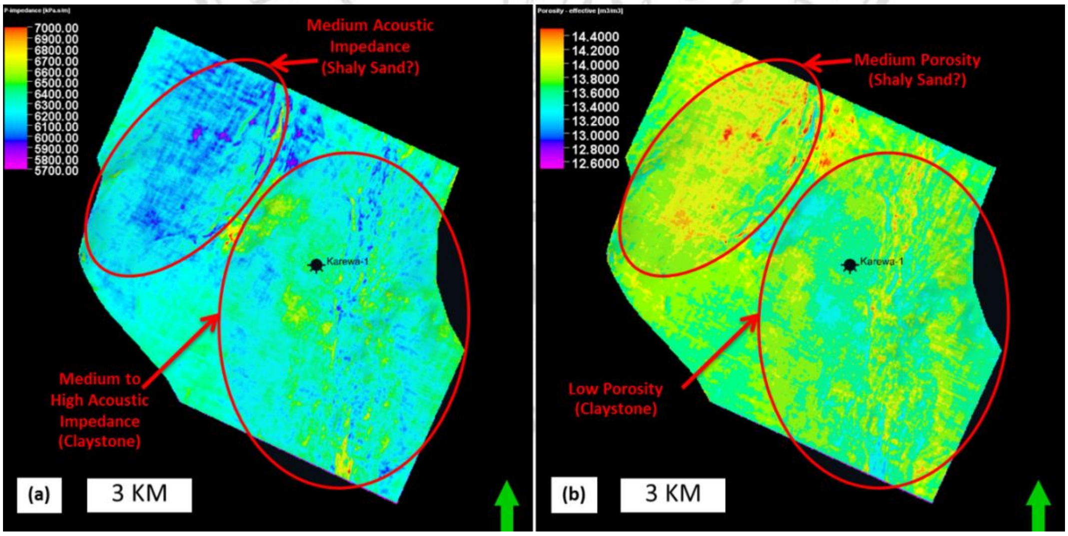

Figure 7-15: H-5 surface distribution maps (a) acoustic impedance, (b) porosity

H-6 was finally interpreted on a prominent positive amplitude reflection (peak) located at 2191ms TWT at well Karewa-1 (inline 1178). The depth is 2485m MD, as derived from the seismic-well tie. The lack of logging data in this depth limits the lithology interpretation at the well position. In Figure 7-16, zones containing high acoustic impedance cover most of the area of H-6, except for the south and SW. These zones are interpreted as shales or claystones. In the south and SW (Figure 7-16), medium to high acoustic impedance is observed with medium porosity. This might be due to a lateral change of lithology between shales and sandstones.

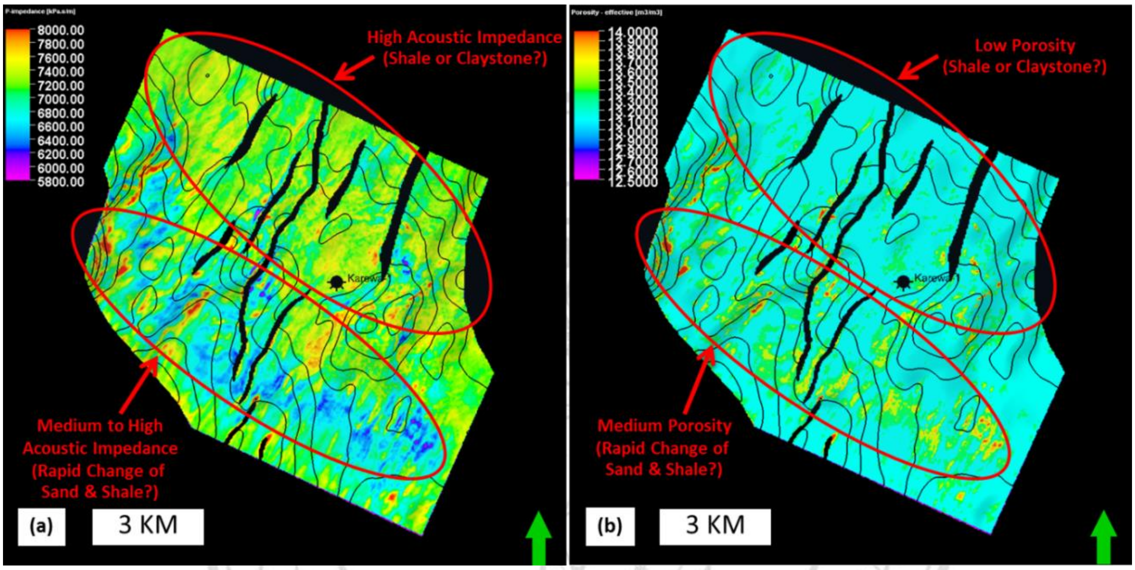

Figure 7-16: H-6 surface distribution maps (a) acoustic impedance, (b) porosity